CONTRACTOR REPORT

NASA CR-66638

NASA CR-66638

WIND TUNNEL CALIBRATION OF THE "ARCASONDE 1-A" AT SIMULATED ALTITUDES BETWEEN 35 AND 56 KM

by E. L. Haak and R. A. Noreen

Prepared under Contract No. NAS 1-7477 *by*
UNIVERSITY OF MINNESOTA, Dept. of Aeronautics and Engineering Mechanics, Minneapolis, Minnesota
for Langley Research Center

NATIONAL AERONAUTICS AND SPACE ADMINISTRATION • WASHINGTON, D.C. • MAY 1968

NASA CR-66638

WIND TUNNEL CALIBRATION OF THE "ARCASONDE 1-A" AT SIMULATED ALTITUDES BETWEEN 35 AND 57 KM

by

E. L. Haak
R. A. Noreen

May 1968

Prepared under Contract No. NAS 1-7477 by
UNIVERSITY OF MINNESOTA
DEPARTMENT OF AERONAUTICS AND
ENGINEERING MECHANICS
Minneapolis, Minnesota
for
NATIONAL AERONAUTICS AND SPACE ADMINISTRATION

WIND TUNNEL CALIBRATION OF THE "ARCASONDE 1-A" AT SIMULATED ALTITUDES BETWEEN 35 AND 57 KM

By E. L. Haak and R. A. Noreen
University of Minnesota

SUMMARY

Results of tests conducted with a full-size "Arcasonde 1-A" atmospheric temperature sensing unit in a low density subsonic wind tunnel are presented. The unit consisted of a 0.25 mm (0.010 in.) thermistor bead mounted on a standard "Arcasonde" instrument package. Equilibrium temperatures of the thermistor bead were measured for Mach numbers from 0.1 to 0.3, and Knudsen numbers from 0.04 to 0.8 in an airstream total temperature with angle of attack and response time to a step change in temperature were also measured at the same flow conditions.

INTRODUCTION

The "Arcasonde 1-A is currently being used to measure atmospheric temperature at high altitudes. It is carried aloft on an Arcas rocket and descends through the atmosphere suspended on a parachute. The resistance of the thermistor bead, a function of temperature, is telemetered back to Earth during the descent using on-board electronics. Although the resistance-temperature relationship of a particular bead is, or can be, accurately determined with no relative motion between the air and the bead, an improvement in the accuracy and reliability of atmospheric temperatures obtained from indicated bead temperatures can be made by determining the effects of relative motion between the air and the bead. In this study some of these aerodynamic effects have been established in a low density subsonic wind tunnel at pressures and velocity conditions identical to those encountered by the sonde during descent. The aerodynamic effects investigated were the thermistor bead equilibrium temperature for a given airstream temperature and velocity, the change in this equilibrium temperature with angle of attack, and the response time of the bead to a step change from an elevated temperature to airstream temperature.

Figure 1a shows the entire nose cone as it is suspended, bead down, beneath the parachute. The thermistor

bead which is about 0.25 mm (0.010 in.) in diameter stands off the mylar mount on its lead wires (Fig 1b).

The authors wish to acknowledge the co-operation of Mr. George Greene, NASA Langley Research Center, and Prof. H. G. Heinrich and Mr. D. J. Horn, University of Minnesota, in the accomplishment of this study.

SYMBOLS

A,B,C	constants in thermistor equation $R = e^{A + \frac{B}{T + C}}$
D	the typical length
K	Knudsen number, λ/D or $1.26\sqrt{\gamma}M/Re$
M	Mach number
P	pressure
ΔP	$P_T - P_S$
T	temperature (°C or °F)
r	recovery factor, $\frac{T_E - T_S}{T_T - T_S}$
R	resistance
Re	Reynolds number based on nominal bead diameter
α	angle of attack
γ	ratio of specific heats
λ	mean free path of the gas molecules
τ	response time
$\delta( )$	the error in a measured or derived quantity

Subscripts:

E	equilibrium conditions
S	static conditions
T	total or stagnation conditions
I	initial conditions

CALIBRATION APPARATUS AND PROCEDURE

In order to (1) provide an instrumentation check-out, (2) validate existing thermistor calibrations, and (3) establish an electrical current level which does not produce a measurable self-heating effect, the thermistors were bench calibrated against a precision mercury-in-glass thermometer at room pressure in a closed container.

Apparatus

Figure 2 is a schematic of the circuit used for measuring the resistance of the thermistor beads. By using the 136 volt battery and the large resistances in series, an extremely stable current could be maintained through the thermistor. This current was set by replacing the thermistor with a resistance of known value and adjusting the voltage drop across it. The differential voltmeter was a five digit type, capable of resolving 10 microvolts or 1 ohm of bead resistance with a 10 microamp current.

Figure 3 shows the bench calibration apparatus. The beads were placed within a brass cup which was in turn placed in a styrofoam insulating container. A partial immersion type mercury-in-glass thermometer was inserted through the cover and provided the reference temperature measurement. Although this system could not be expected to provide stable temperatures throughout a wide range, the room temperature range was of primary interest in this study and in this area the system was quite adequate. Using heating tapes wrapped around the brass cup, temperatures up to 65°C (150°F) were obtained, and by removing the tapes and placing ice water in the container, points near 0°C could be obtained.

Calibration Results

Self-heating.- Initial resistance measurements were made with bead currents of 0.5, 5, and 10 microamps, which, with a bead resistance of about 10K ohms, correspond to power dissipations of 0.0025, 0.25, and 1 microwatts. Results of these measurements showed identical resistance values for the three bead currents at any given temperature indicating that electrical currents of this magnitude do not cause resistive heating in the thermistor. A 10 microamp current was used for subsequent tests, since the higher current essentially gives an increased sensitivity in the voltage measurement.

Bead resistance and temperature.- The thermistors used in this study were supplied by the sponsoring agency along with calibration curves which were established by the manufacturer. These calibration curves were derived from measurements of temperatures and resistances at 35°, 0°, -25°, and -65°C. A "standard thermistor curve" was then drawn through these four points. After initial bench calibration showed a discrepany of 0.5°C or greater with the furnished data at room temperature (~22°C), the constants in the equation

$$R = e^{A + \frac{B}{T + C}}$$

were re-evaluated using the manufacturer's calibration points at 35°, 0°, and -25°C. With these constants, a new calibration curve was constructed by calculating resistance values for 0.5°C temperature intervals. A comparison of the bench calibration data with the reconstructed calibration curve for bead No. 4418 (Fig 4) shows excellent agreement throughout the test range. Using the same procedure for bead No. 4417 gave agreement similar to that shown in Fig 4. This procedure, however, was not satisfactory for the third bead No. 4955, suggesting that perhaps one of the manufacturer's calibration points was in error. Therefore, it was calibrated against the thermometer and bead No. 4417 through the room temperature range.

Calibration Error

An error analysis for this calibration procedure is contained in Appendix A. From the results of this analysis and in view of the agreement with the manufacturer's calibrations, the maximum possible calibration errors appear to be less than 0.1°C.

WIND TUNNEL STUDIES

The aerodynamic effects investigated in the low density wind tunnel were the equilibrium temperature of the thermistor bead, T_E, for a given airstream temperature, the variation in T_E with angle of attack, α, and the response time, τ, of the bead of a step change in temperature all as a function of velocity and pressure level. This section describes the wind tunnel, apparatus, and test procedures for the three types of tests conducted.

The Low Density Wind Tunnel

The continuous flow low density wind tunnel is shown in Fig 5. It is a closed circuit horizontal return type, capable of operating at Mach numbers up to 0.9 and at reduced speeds will operate at pressures down to 0.25 torr. The tunnel has an open-jet test section with various interchangeable subsonic nozzles for gross changes in air speed, with finer adjustments in velocity made using a butterfly throttling valve located on the downstream side of the driving compressor. The tunnel leak rate of 0.1 torr/min is sufficiently small to allow quasi-steady state operation without vacuum pump operation at any but the lowest pressures. True steady state conditions are obtained by balancing the pumping rate with the leak rate at a particular pressure. In this test series, the vacuum pump was operating for data points at pressures of 1 torr and below.

While the air pressure and airstream velocity can be controlled, the airstream temperature cannot. During the initial evacuation of the tunnel circuit from local atmospheric pressure, there is a rapid decrease in air temperature from room temperature to below 0°C caused by the expansion of the air within the tunnel. After passing the maximum pumping rate, the air in the tunnel begins warming nearly as rapidly because of conductive heat transfer from the air in the room and the steel tunnel walls. The tunnel can be evacuated from local atmospheric pressure to minimum pressure in 15 minutes; by this time the air temperature has cooled and returned to within 2°C of room temperature, and after about 30 minutes the air in the tunnel has returned to equilibrium within 0.1°C of the tunnel wall temperature. Subsequent evacuations from pressures of 10 torr or less to minimum pressure produce temperature changes of less than 0.5°C and air temperature returns to wall temperature in less than five minutes. Thus after an initial evacuation and sufficient delay to reach equilibrium, the air temperature is essentially constant at wall temperature.

The previous discussion dealt with preliminary "no-flow" temperatures, that is, the driving compressor was not operating and the air was not being forced around the tunnel circuit. If, after the initial evacuation and delay to reach equilibrium, the driving compressor is started and flow established, the airstream temperature is within 0.5°C of wall temperature. For pressures in the range of interest for this study, this airstream temperature then increases at about 0.2°C/hour due to the frictional heating of the moving air.

In summary then, this facility provides a controlled steady state velocity and pressure and when properly operated, a reasonably steady airstream temperature is available.

Thermistor Equilibrium Temperature

The objective of this phase of testing was to determine the bead equilibrium temperature in the Mach number range from 0.10 to 0.30 for altitudes between 48,750 m (160,000 ft) and the maximum altitude attainable in the wind tunnel. The relationship between thermistor equilibrium and airstream temperatures is conventionally expressed in terms of recovery factor, r, where

$$r = \frac{T_E - T_S}{T_T - T_S}$$

and the difference between total temperature, T_T, and static temperature, T_S, is an established function of the airstream Mach number (Ref 1).

Figure 6 shows the wind tunnel installation. Figure 7a is a photograph of the test section and instrumentation while Fig 7b is a close-up of the test section interior. The full-scale "Arcasonde" without the battery pack was suspended in the flow. Mass flow requirements of the wind tunnel operation dictated a nozzle with a 5 in. exit diameter, hence, the large blockage from the sonde could not be avoided. However, it is not felt that this was severely restrictive since the region of primary interest was the immediate area around the bead. The open-jet design allows the flow to expand around the nose cone maintaining satisfactory flow at the bead and mount. To determine Mach number, total pressure was measured on a Stokes portable McLeod gage and the difference between total and static pressures was measured with a MKS Baratron differential pressure sensor. One of the thermistor beads was placed in the near stagnation region upstream of the nozzle (Fig 6) and used for a total temperature sensor. The two bead resistances were measured simultaneously in exactly the same manner as described in the section on calibration apparatus and procedure.

The reasons for using a thermistor bead for a total temperature sensor must be explained, since at first glance it appears that the item to be calibrated was used as a reference. At the start of this investigation, total temperature was to be measured in the flow downstream of

the nozzle exit with a conventional total temperature probe, which had the normal shielding and produced a near stagnation region around a small thermocouple element. Such a probe was calibrated along with the beads, installed in the tunnel and preliminary tests made; results were totally unacceptable and inexplicable. After considerable difficulty, experimentation, and elimination of various possible causes of the errors, it was concluded that the response time of this relatively massive probe at pressures below 5 torr was much longer than the rate of change of the wind tunnel air temperature.

The possibility of designing and constructing a conventional shielded total temperature probe with a sufficiently short response time was ruled out, since this new probe would require response characteristics similar to those of the test thermistor. The only reasonable method of measuring reference total temperature, where the response time was assuredly short, was to place one of the thermistor beads upstream of the nozzle. Considering the area ratio of the nozzle, the maximum velocity upstream of the test section for these tests is in the order of 20 fps. At this velocity, the difference between total and static temperature is less than 0.03°C. In view of this small difference, a probe without any type of stagnation producing shroud placed upstream of the nozzle would provide a sufficiently accurate measurement of total temperature if its response time was short enough. Therefore, one of the thermistor beads was used since its response time was considerably shorter than anything else available.

Change in Angle of Attack

The "Arcasonde" without the battery pack was mounted on a motor driven, remotely operated rotating mechanism (Fig 8). The sonde was positioned on this device such that the thermistor bead was on the wind tunnel centerline and also on the axis of rotation of the system. Thus, the bead remained at approximately the wind tunnel centerline for all angles of attack.

Test data was taken at wind tunnel pressure levels of 0.25, 0.50 and 1.00 torr with angles of attack of 0, $\pm$10°, 20° and 30°. The angle of attack was varied throughout the range several times. The angle settings were obtained by viewing the angle indicator through the test section window and operating the mechanism by remote control. Therefore, the entire study was performed without interruption for mechanical changes or changes in wind tunnel pressure level.

Time Constant Studies

An evaluation of the time required for the bead to respond to a change in air temperature is needed to determine the time required for the bead to reach equilibrium temperature after the protective nose cone is separated from the instrument package, and to establish the capability of the thermistor to sense variations in atmospheric temperature. In these tests the thermistor and upper end of the sonde were totally enclosed in a wind shield which contained electrical heating elements. The electrical heater-air shield (Fig 9) was a split brass cup with Nichrome wire heaters and insulation on the outside. Each half of the heater had a support beam which pivoted at bearings mounted on the cover of the angle of attack changing mechanism, allowing each half of the heater to be rotated out of the flow independently. The heater halves were then held together against the tension of retracting springs by a fine high resistance wire which was disintegrated electrically at test initiation. In a typical test sequence, the wind tunnel was adjusted to the desired velocity and pressure level and the thermistor output was monitored until it indicated a steady temperature approximately 40°C above ambient conditions, at which time the test was initiated by burning the restraining wire. The transient output from the thermistor was fed through a DC amplifier which replaced the differential voltmeter in the resistance measuring circuit and was recorded on a light beam oscillograph, giving a continuous trace of bead resistance with time, after the heated bead had been exposed to the flow. Time constant determination tests were conducted at Mach numbers of 0.1, 0.2, and 0.3 at pressures of 0.3, 0.5, and 1.0 torr at each Mach number.

In earlier tests, it was established by high speed motion pictures, 2,000 frames/sec, that the lapsed time for the heater shroud retraction was 0.025 sec. or less. In view of the thermistor response times shown in the next section, this time increment is considered negligible.

RESULTS

Thermistor Equilibrium Temperature

All actual test data is presented in Fig 10 and tabulated in Appendix B with $T_T - T_E$, the difference between the measured temperatures, as a function of static pressure or altitude. These altitudes and all others in this report are based on the pressure and geometric

altitude relationships tabulated in Ref 2, and they have been included for reference only. Since initial tests indicated a relatively large variation in equilibrium temperature with static pressure, additional data was obtained at Mach 0.3 through a wider range in pressures, and it is felt that this curve may be used as somewhat of a guideline for interpolating the results at other Mach numbers. The data included in Fig 10 and later in Fig 11, have been assembled from two test sequences. The solid symbols are initial data while the open symbols are data from the later angle of attack studies.

In order to compare these results with other published data of essentially the same type (Refs. 1, 4, and 5), the temperature differences have been ratioed to the difference between total and static temperature at the respective Mach numbers yielding the conventional recovery factor, r, where

$$r = \frac{T_E - T_S}{T_T - T_S}$$

The recovery factor plotted versus Knudsen number is shown in Fig 11, with the Knudsen number, K, defined as:

$$K = \frac{\lambda}{D}$$

where λ is the mean free path, and D is a typical length, which, in this study, is the thermistor bead diameter, 0.25 mm (0.010 in.). The Knudsen number can also be expressed in terms of the Mach and Reynolds numbers (Ref 3):

$$K = 1.26\sqrt{\gamma}\frac{M}{Re}$$

The Knudsen numbers presented in Fig 11 were calculated using this expression and $\gamma = 1.4$ for air.

Again using the M = 0.3 data as a guide, it can be seen that a change from the practically constant recovery factor in continuum flow to recovery factors greater than unity in the region between continuum and free molecular flow is evident at all Mach numbers. Similar results are shown in Refs 4 and 5 and are indicated in Figs. 12a and 12b. The data in both of these figures was from tests at supersonic speeds, with Fig 12a (Ref 4) for spheres and Fig 12b (Ref 5) for transverse cylinders. The data obtained in this study at subsonic speeds is represented in Figs 12a and 12b by a curve which is a first approximation to the data in Fig 11.

The comparison shows good agreement of general trends, a constant recovery factor for $K < 0.1$, then increasing almost linearly, on a semi-logarithmic plot, to values greater than unity. With this agreement of trends between this newly established subsonic data and supersonic data, from existing literature, and noting that all of the test data from this study fits the trend of the $M = 0.3$ data within the error limits, it appears that the recovery factor is primarily a function of Knudsen number. On the other hand, Ref. 1 shows that in accordance with theoretical calculations the recovery factor varies with Mach number in true free molecular flow. Recovery factors of about 1.5 for a Mach number of 0.5 are predicted which increase to approximately 1.6 as the Mach number approaches zero. This suggests that at given Knudsen numbers of 1.0 and greater, there may be a slight increase in recovery factor with decreasing Mach number. While these variations in recovery factor with Mach number may seem significant, it should be noted that these variations represent extremely small temperature differences in the low subsonic flow regime, and in order to retain the proper prospective from this standpoint, a scale is also included in Fig 11 showing the variation in recovery factor for 0.1°C at each of the test Mach numbers. This scale also furnishes an approximate gage for the estimated errors, which are treated in greater detail in Appendix A.

Temperature Variation with Angle of Attack

The results of the equilibrium temperature measurements at angles of attack from -10° to 30° are shown in Fig 13 with $T_T - T_E$ as a function of angle of attack. Tests were conducted at Mach numbers from 0.1 to 0.25 at constant total pressures of 0.25, 0.5, and 1.0 torr. The tests at $M = 0.3$ were made at 0.3, 0.5, and 1.0 torr due to facility limitations. The data points at $\alpha = 0$ were presented earlier in terms of recovery factor (Fig 11). The data in Fig 13, however, presents the measurements in terms of temperature differences, since the procedure of dividing nearly equal small differences magnifies any changes. Figure 13 shows that the changes in T_E due to angle of attack are generally small, that is, within the 0.1°C error. However, there are discernible trends of a slight decrease in T_E with angle of attack for the lower Mach numbers, changing to a distinct increase in T_E at higher Mach numbers for $\alpha = 20°$ and $\alpha = 30°$. At the present time, this effect cannot be fully explained; however, one should recall that the nose cone was relatively large for the 5 in. nozzle, and although there was no observable changes in

total or static pressure due to an angle of attack change, some variation in the bead flow field cannot be disregarded as a possible cause.

Response Times

Thermistor responses to changes in temperature were evaluated at Mach numbers of 0.1, 0.2, and 0.3 and pressures of 0.3, 0.5, and 1.0 torr. The response time, τ, is defined as the time period required for the bead temperature to decrease from an initial value, T_I, to a temperature, T, where

$$\frac{T - T_E}{T_I - T_E} = \frac{1}{e}$$

Figure 14a is a typical oscillogram of bead resistance change with time. Since the relationship between bead resistance and bead temperature is not linear, the ordinates in Fig 14a are, of course, not proportional to temperature. Figure 14b and Table 1 show the results of the response time tests versus Mach number with the total pressure as parameter. It is noticed that the most rapid responses occur at the high velocity-high pressure conditions.

APPENDIX A

ERROR ANALYSIS

The possible errors involved in the final results can be divided into two categories, temperature measurement errors including calibration errors, and the errors in determining flow conditions.

Errors in Temperature Measurements

Calibration error.- Errors in the calibration can arise from two general sources, first errors in resistance measurements, and second, errors in reference temperature measurement.

Resistance measurements: The bead resistance was obtained by measuring the voltage across the bead with a known current passing through the bead. This bead current was set by adjusting the measured voltage drop across a resistor of 19,810 ohms $\pm$ 10 ohms, measured with a precision wheatstone bridge. The differential voltmeter was commercially calibrated before testing began, and certified that the calibration was traceable to the National Bureau of Standards and that the instrument was within manufacturer's specifications of $\pm$ 50 microvolts or 0.1% of input whichever is greater, for measurements in the present range of interest. Thus the total error in resistance measurement is 0.25%, with 0.05% error from the precision resistor and 0.20% error from the two voltage measurements necessary. Assuming a nominal bead resistance of 10,000 ohms gives an error of $\pm$ 25 ohms or, using the slope of the calibration curve in Fig 4, $\pm$ 0.07°C.

Reference temperature error: Error in the reference temperature measurement cannot be determined as precisely as error in the resistance measurement. The mercury-in-glass thermometer was ruled in intervals of 0.2°F and could be read to within 0.05°F (0.03°C) quite readily. As mentioned previously, the indicated temperature of a mixture of crushed ice and water was checked and was 32.00°F, but no other accuracy information was obtained. Assuming that the thermometer inaccuracy is less than the reading error would result in an over-all calibration error, from resistance and temperature measurement, of about $\pm$ 0.1°C. This result appears consistent with agreement obtained in Fig 4; the equation used to calculate

resistance values should be accurate to better than ± 0.1°C through the limited range, and the manufacturer's calibration points are supposedly more accurate, except for what is apparently an inadvertent mistake on one of the thermistor beads. On this basis, the calculated resistance and temperature relationships were used as calibration curves, except in one case where one bead was calibrated against another, and the over-all error in temperature measurement is felt to be less than ± 0.1°C.

Equilibrium and total temperature errors.- From the discussion above, the reasonable error in a single temperature was found to be less than 0.1°C. Using this, the error in the difference between two measured temperatures could be 0.2°C. However, the spread of the data presented is considerably less than 0.2°C, in fact, it is generally less than 0.1°C. Thus the error of ± 0.2°C appears to be an indication of the maximum possible randome error, while a more realistic estimate of actual errors in temperature differences would be ± 0.1°C.

Errors in Flow Condition Measurement

Two quantities were measured to determine the flow conditions, total pressure and the difference between total and static pressure. The errors in these quantities are obtained from instrument errors, and the corresponding errors in Knudsen number can be calculated.

Total pressure was measured with a Stokes portable McLeod gage, while, again, no accuracy information was contained in the specifications, the gage was kept at a pressure of 10^{-3} torr when not in use and agreed with other vacuum gages available. From these checks, the reading error of the McLeod gage of ± 0.01 torr for the range of test pressures seems to be the best estimate of error.

The error in the MKS Baratron instrument used for measuring the difference between total and static pressures, ΔP, was 2×10^{-4} torr, from the manufacturer's specifications.

Errors in Mach and Reynolds numbers caused by errors in pressure measurement have been found in Ref 6 to be

$$\frac{\delta M}{M} = \frac{1}{2}\left[\frac{\delta P_S}{P_S} + \frac{\delta P}{P}\right]$$

$$\frac{\delta Re}{Re} = \frac{1}{2}\left[\frac{\delta P_S}{P_S} + \frac{\delta P}{P}\right]$$

excluding any error due to temperature measurement or typical length. From this it is obvious that the largest errors occur at the lowest pressure and lowest Mach number, but because the very slight changes in T_S/T_T at the low Mach numbers, the highest errors in $T_T - T_S$ will occur at the highest Mach number and lowest pressures. On this basis then, the following table was constructed using the instrument errors and the above equations.

M	P_S(torr)	ΔP	$\frac{\delta M}{M}$ & $\frac{\delta Re}{Re}$	δM	ΔT_S	$\frac{\delta K}{K}$
0.1	0.25	0.0018	0.08	$\pm$0.008	$\pm$0.08°C	$\pm$0.16
0.3	0.30	0.0181	0.02	$\pm$0.006	$\pm$0.20°C	$\pm$0.04

The term ΔT_S represents the change in static temperature due to the change in Mach number, δM, assuming a constant total temperature. Combining all possible errors into one over-all error in recovery factors yield a maximum possible error in excess of 150 per cent, which is obviously due to the form of the recovery factor definition involving the division of two small differences. However, the actual spread of temperature data shown in Fig 10 indicates that over-all accuracies of presented results are considerably better than the estimates of maximum possible error predict.

Since the Knudsen number is a function of M/Re, the error in Knudsen number, $\delta K/K$, shown in the above table is expressed as

$$\frac{\delta K}{K} = \frac{\delta Re}{Re} + \frac{\delta M}{M}$$

The 4 per cent error at higher Mach numbers would have little effect on the results; the 16 per cent error at low Mach numbers and pressures is high, but nearly unavoidable considering the nature of the measurements.

Error Summary

The discussion above provides an estimate of the maximum possible error in temperature and flow

measurement, but with no consideration for test technique, experimental procedure and statistical evaluation. Therefore, while the calculated possible errors above are generally not excessive, particularly in view of the quantities measured, it is felt that the actual errors incorporated in the presented results are much smaller than the maximum values predicted above. This statement appears to be well supported considering the point to point agreement of the data and their agreement with data in other publications.

APPENDIX B

WIND TUNNEL DATA AND THERMISTOR CONSTANTS

This section includes all of the wind tunnel data for the equilibrium temperature tests and the angle of attack studies (Table 2, p. 32).

The constants for the thermistor equation, used to define the resistance-temperature relationship, $R = e^{A + \frac{B}{C + T}}$, (T in °C) for the two thermistors used in the testing are given below:

Thermistor No. 4417 (R_E)

A = -4.46379

B = 4856.5434

C = 330.7641

Thermistor No. 4955 (R_T)

A = -4.40326

B = 4856.5434

C = 330.7641

REFERENCES

1. Ames Research Staff: Equations, Tables, and Charts for Compressible Flow, NACA TR 1135, 1953.

2. U. S. Standard Atmosphere 1962. Washington, D. C., December, 1962.

3. Schaaf, S. A.; and Chambre, P. L.: Flow of Rarefied Gases. Princeton University Press, Princeton, New Jersey, 1961.

4. Koshmarov, Y.; et. al: Heat Transfer and Equilibrium Temperature of a Sphere in a Supersonic Flow of Rarefied Gas. Translated from Academy of Science U.S.S.R., Bulletin of Fluid and Gas Mechanics, No. 4, pp. 175-177 (1966) by John Hopkins University, AD 652 820.

5. Drake Jr, R. M.; and Backer, G. H.: Heat Transfer from Spheres to a Rarefied Gas in a Supersonic Flow. Annual Meeting ASME, Atlantic City, N. J. Paper No. 51-A-55, 1951.

6. Touryan, K. J.; and Drake Jr, R. M.: Flow Investigation in Delaval Supersonic Nozzles at Very Low Pressure. Vol 2 of Rarefied Gas Dynamics, J. A. Laurmann, ed., New York-London, 1963.

7. Oppenheim, A. K.: Generalized Theory of Convective Heat Transfer in Free Molecule Flow. J. Aeron. Sci., Vol. 20, No.1, 1953.

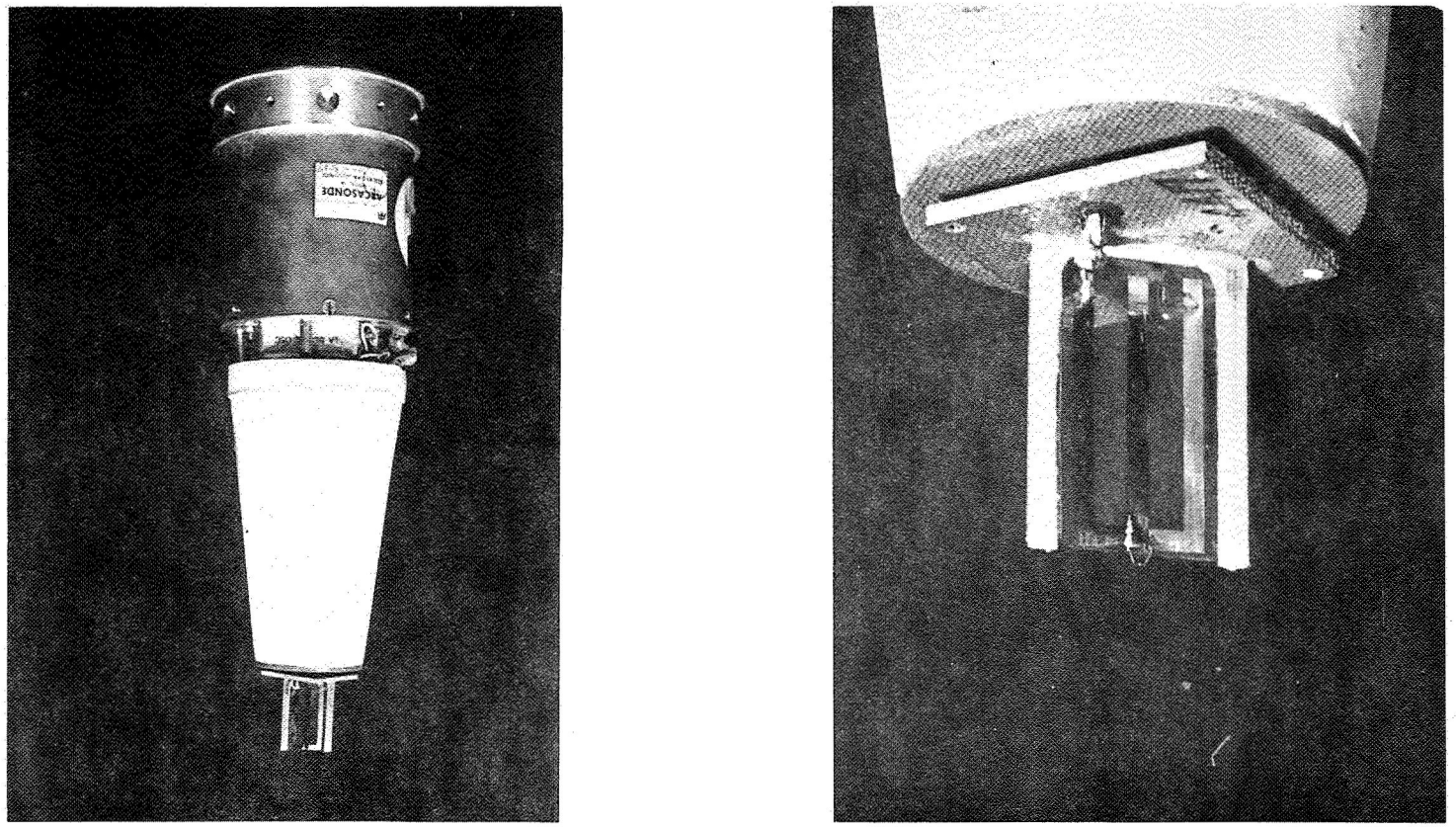

(a) (b)

Fig 1 The Sensor Unit and Thermistor Bead

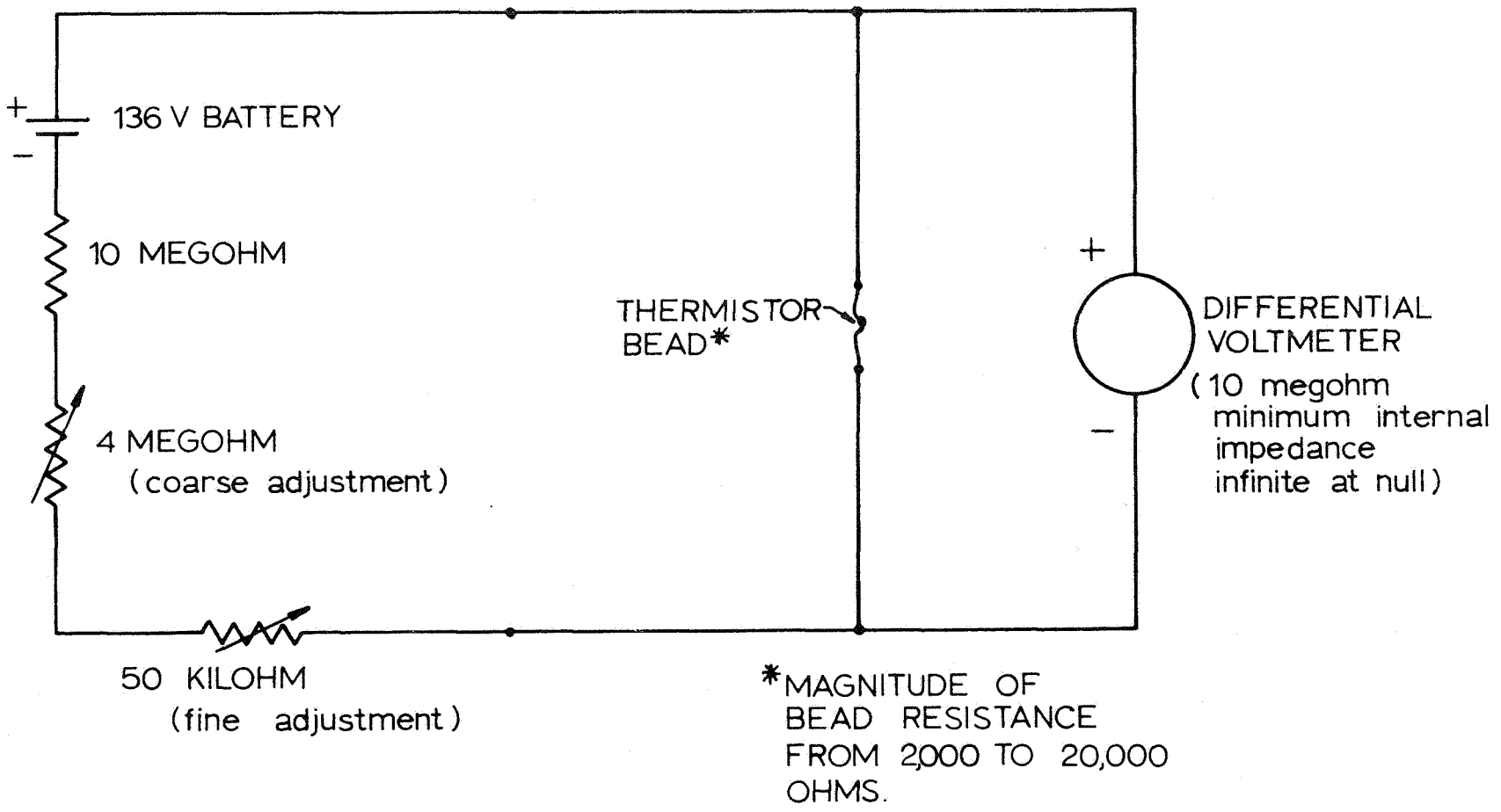

Fig 2 Schematic of Resistance Measuring Circuit

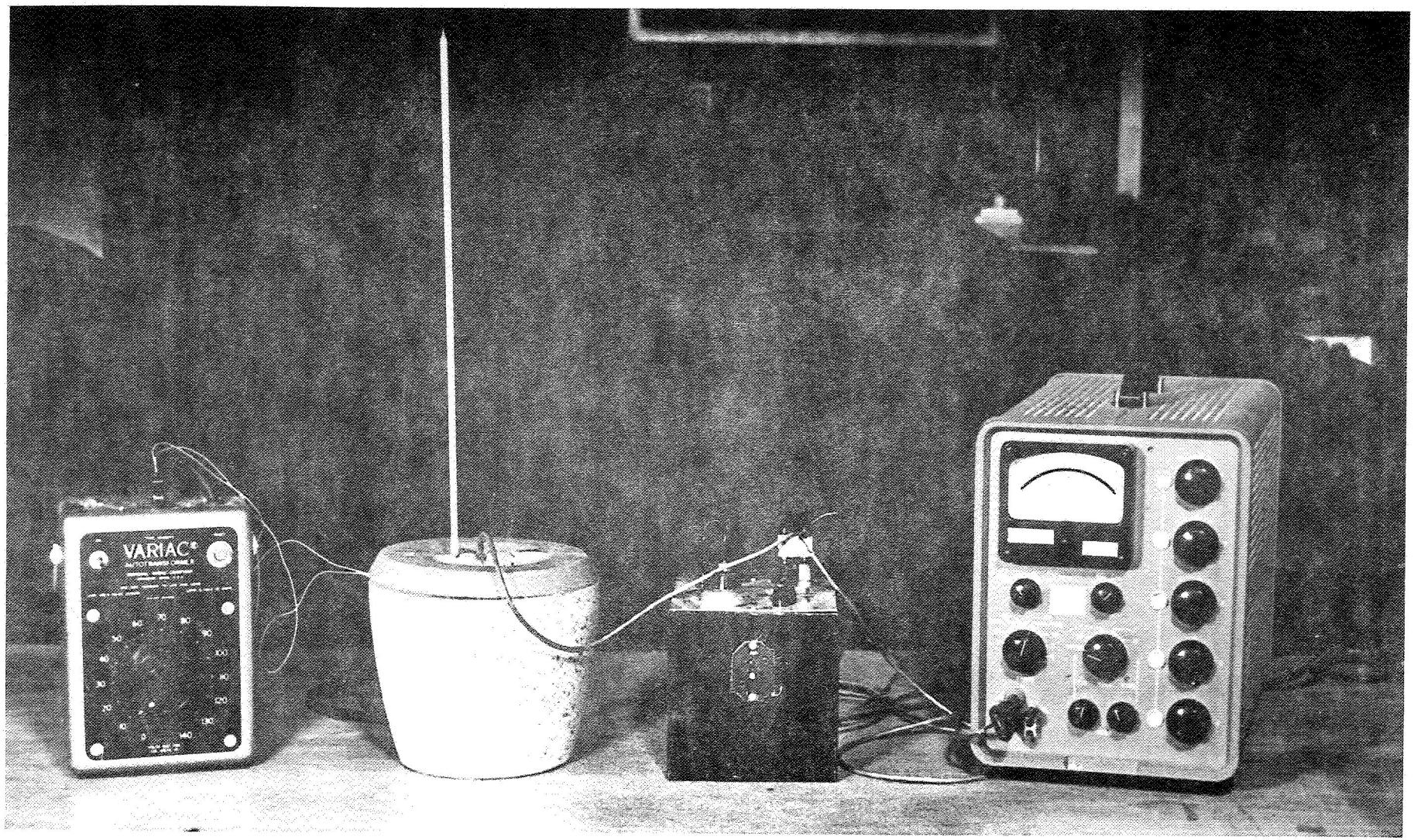

Fig 3 Bench Calibration Apparatus

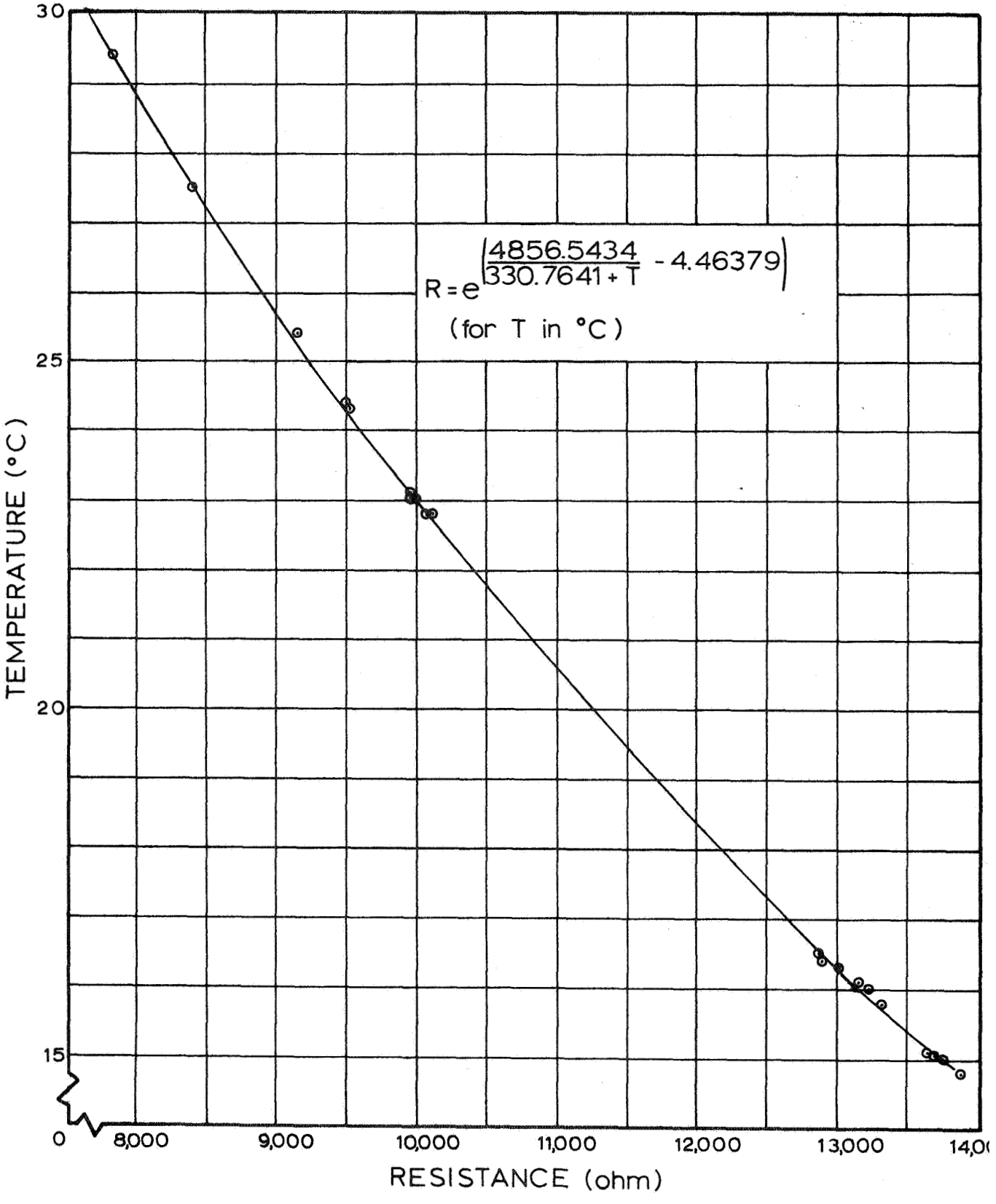

Fig 4 Calibration Curve, Bead 4418

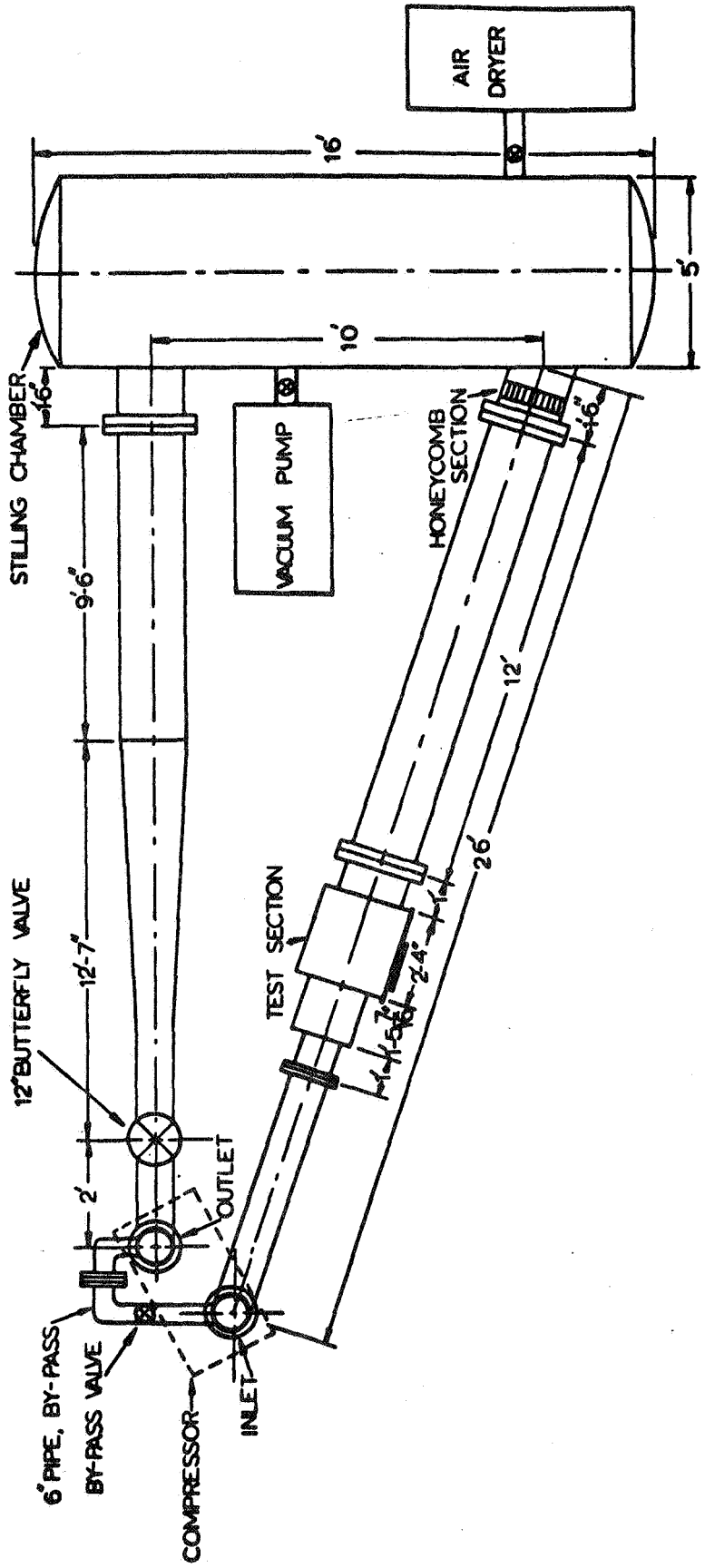

Fig 5 Low Density Wind Tunnel

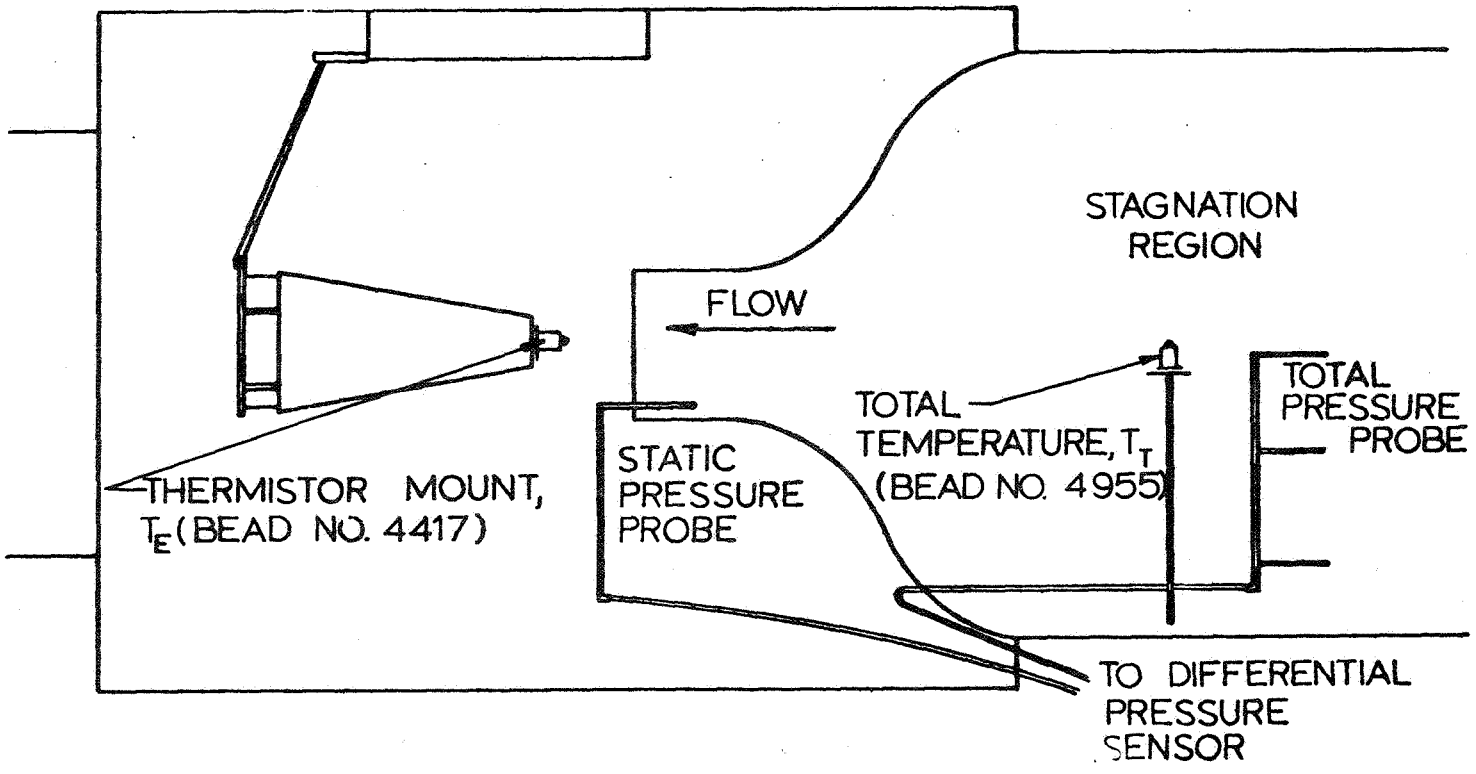

Fig 6 Schematic of Wind Tunnel Installation

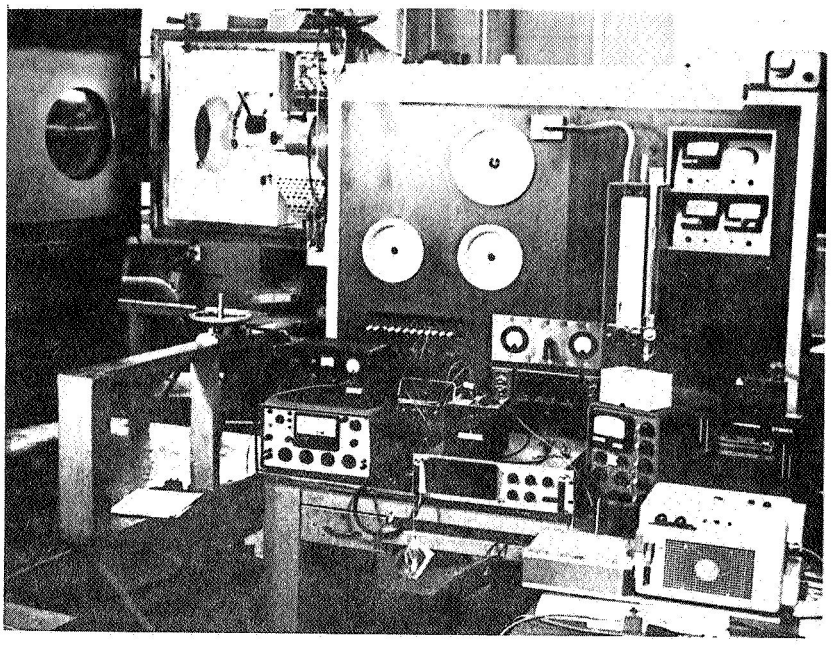

(a)

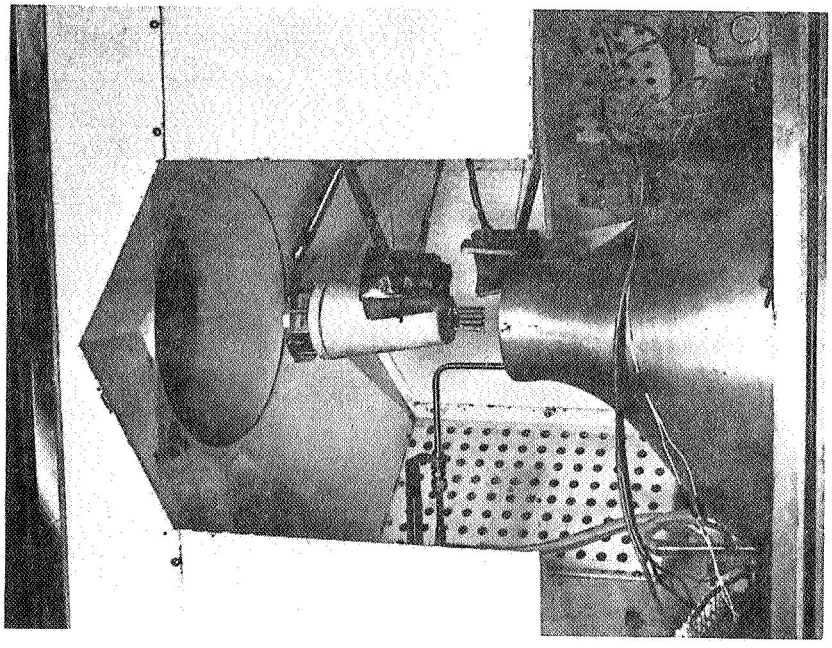

(b)

Fig 7 Wind Tunnel Instrumentation and Test Section Interior

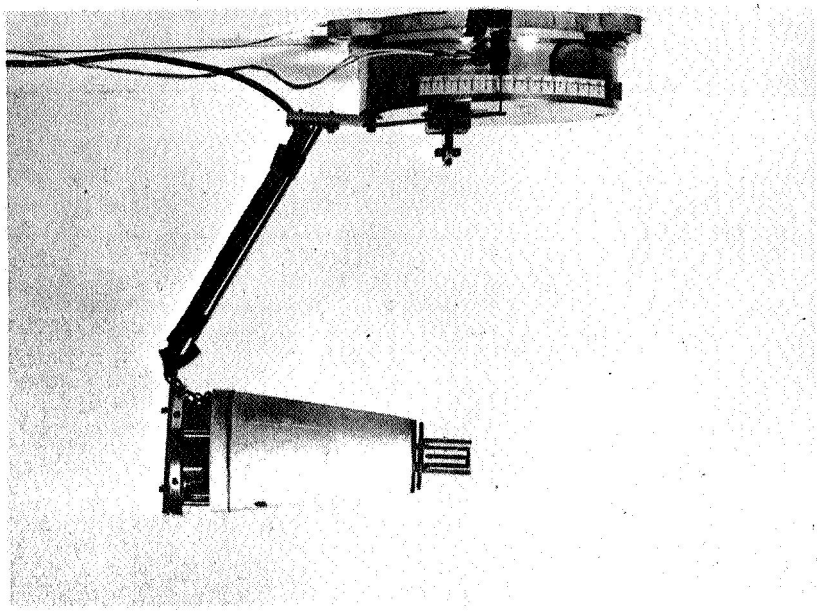

Fig 8 Angle of Attack Positioning Mechanism

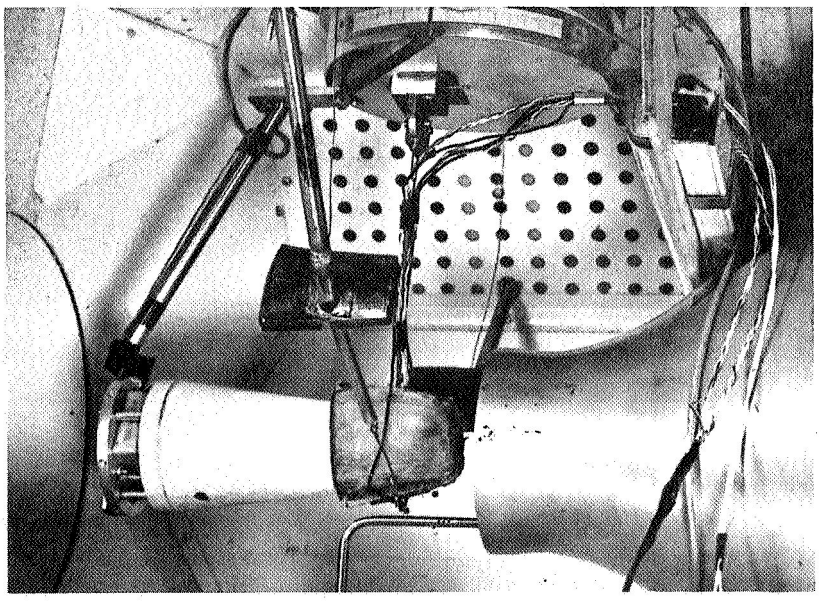

Fig 9 Removable Heaters in Heating Position

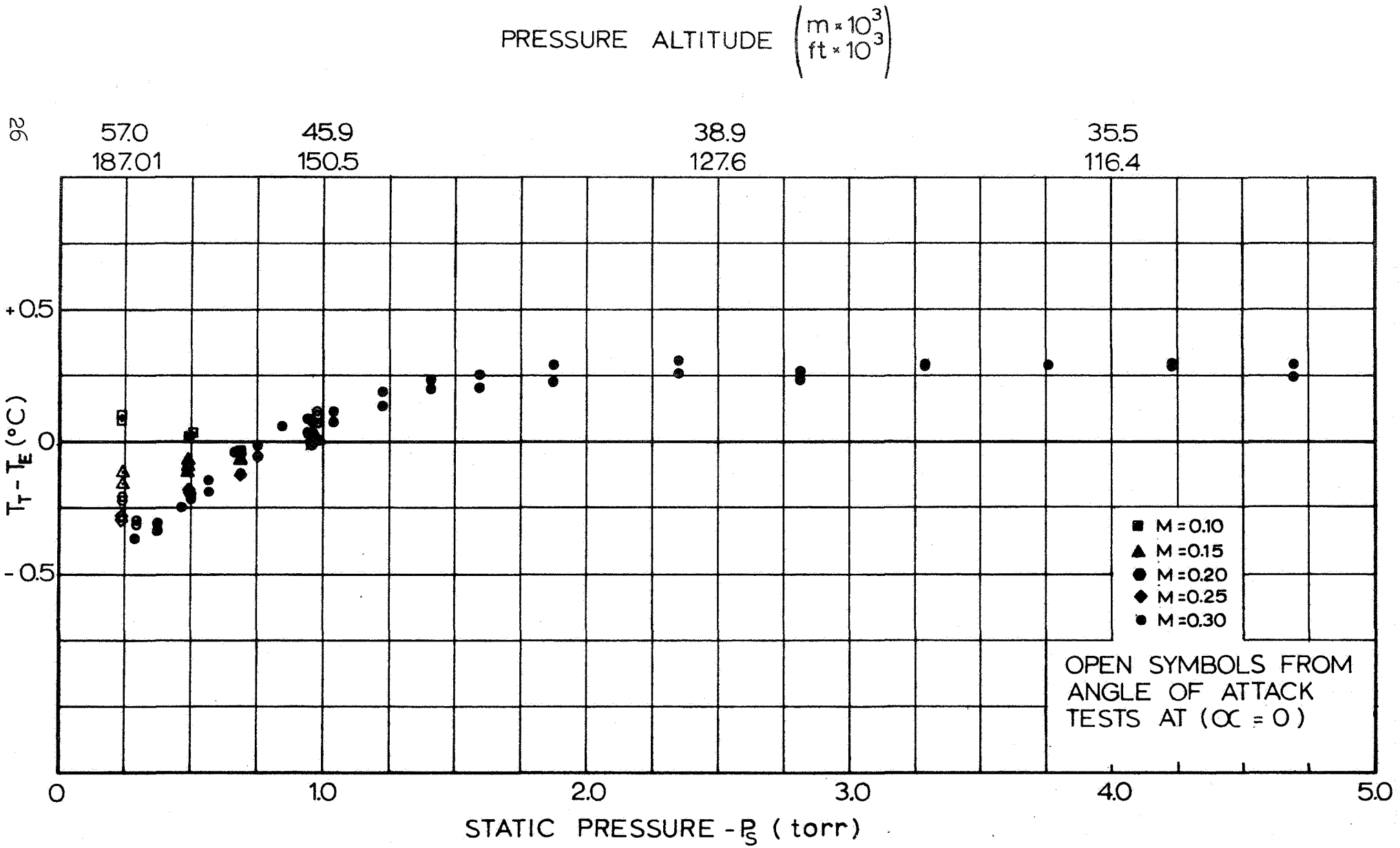

Fig 10 $T_T - T_E$ as a Function of Static Pressure ($\alpha = 0$)

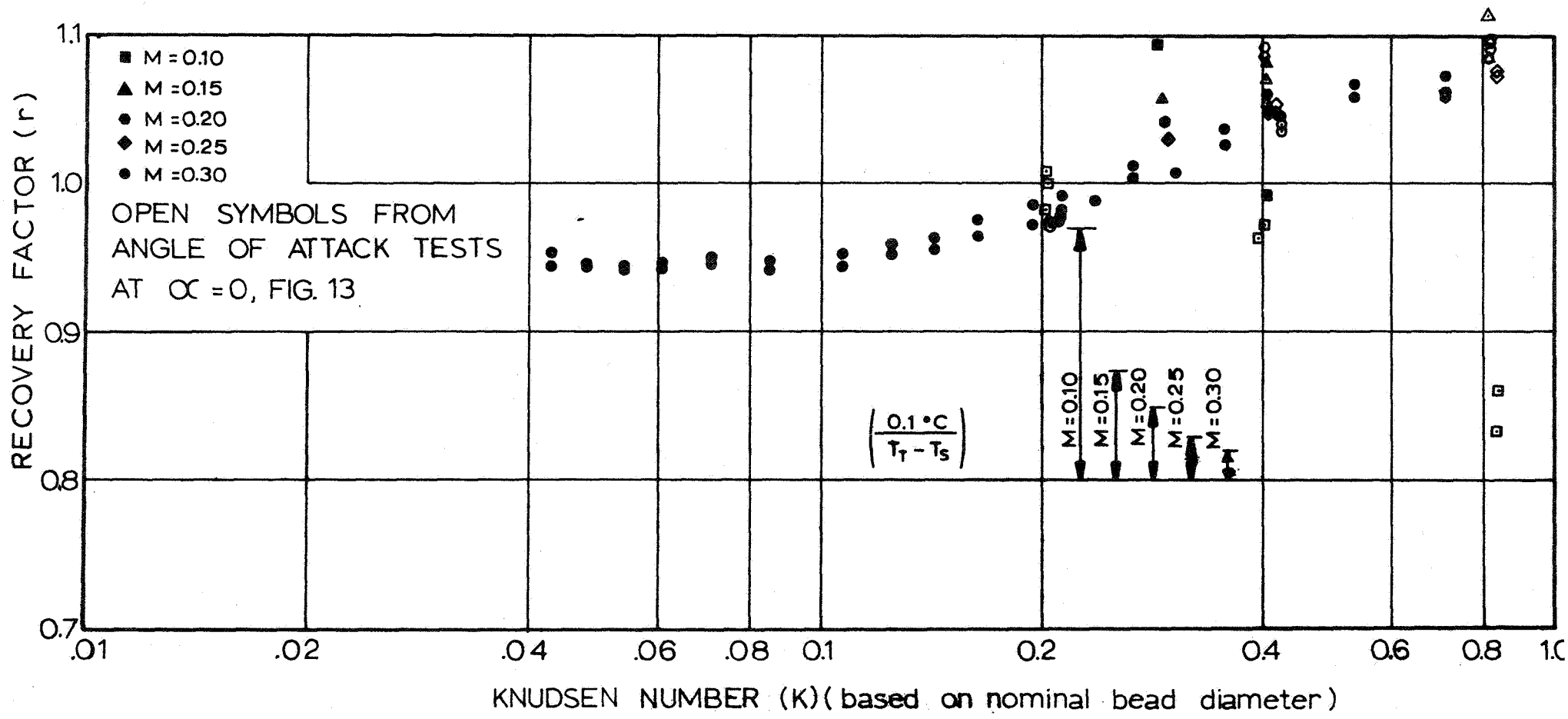

Fig11 Thermistor Recovery Factor as a Function of Knudsen Number (OC = 0)

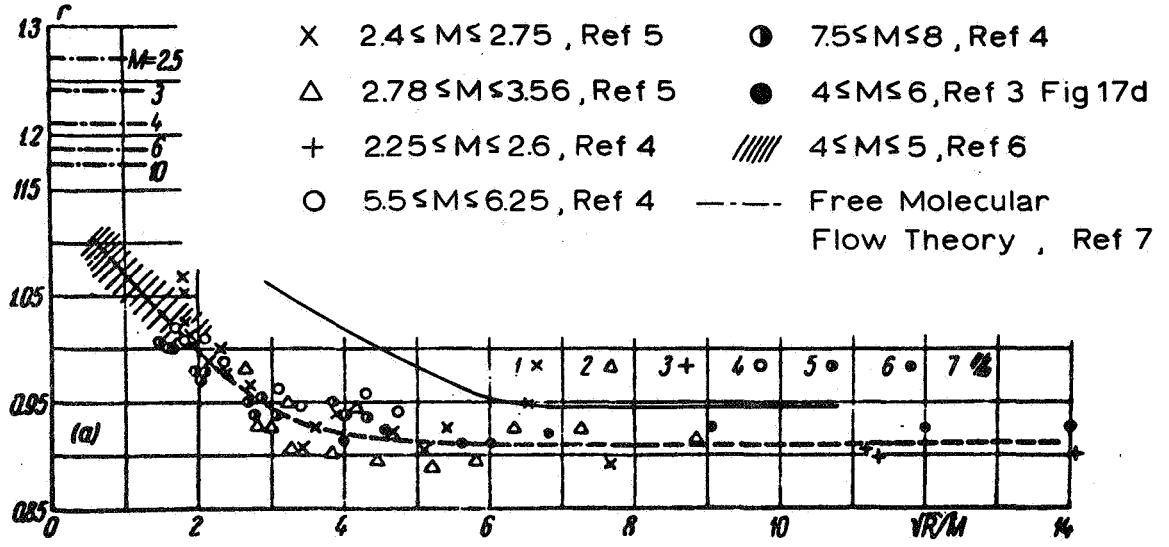

FIGURE 12a RECOVERY FACTOR VS $\sqrt{R_e}/M$ FOR SPHERES IN SUPERSONIC FLOW (TAKEN FROM REF. 4)

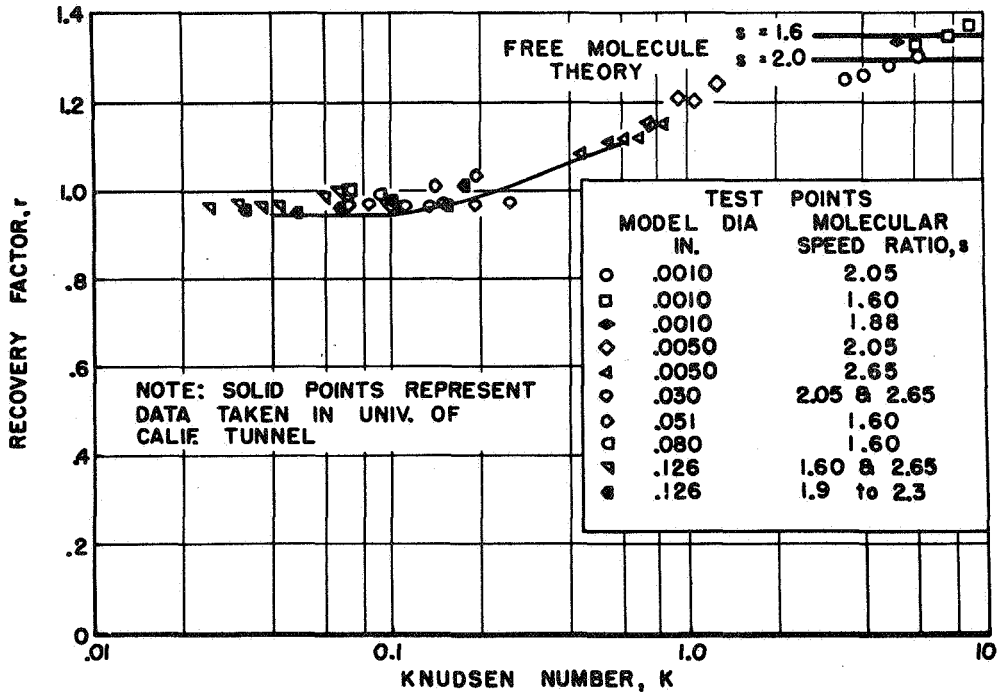

FIGURE 12b VARIATION OF RECOVERY FACTOR WITH KNUDSEN NUMBER. FOR TRANSVERSE CYLINDERS IN SUPERSONIC FLOW (TAKEN FROM REF. 5)

NACA

NACA TN 2438

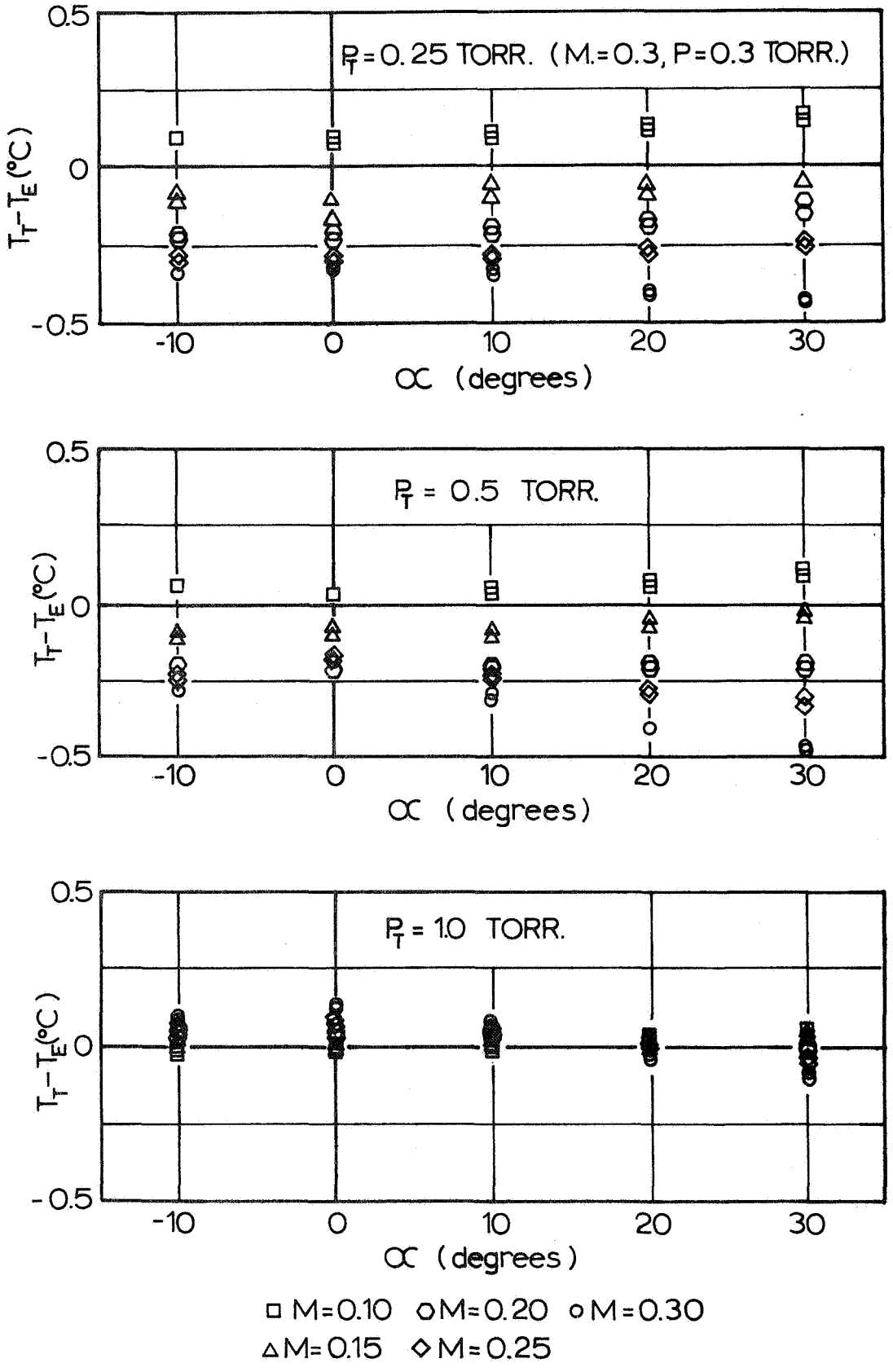

Fig 13 T_T-T_E as a Function of Angle of Attack for Various Total Pressures

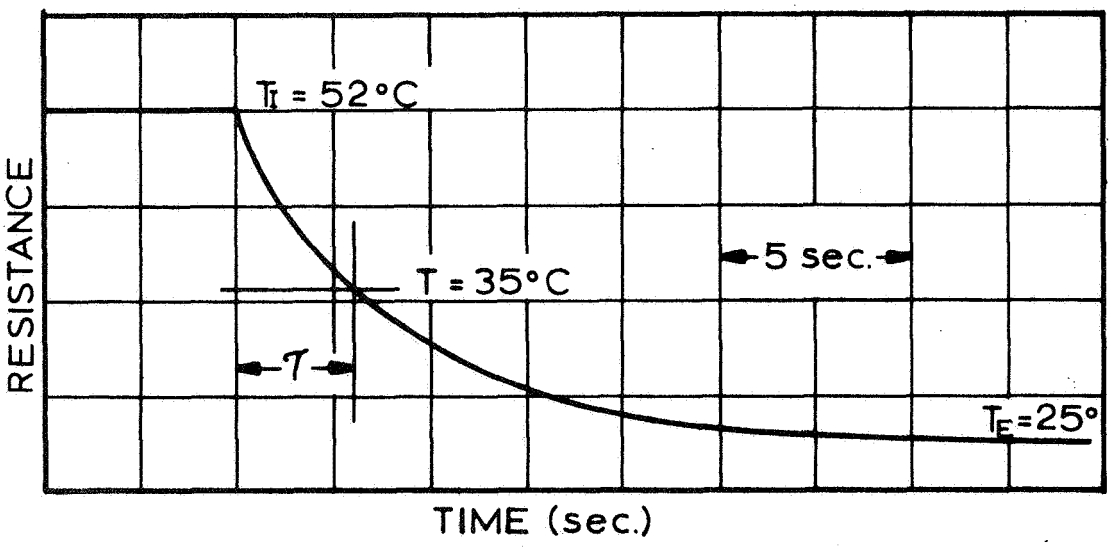

(a)

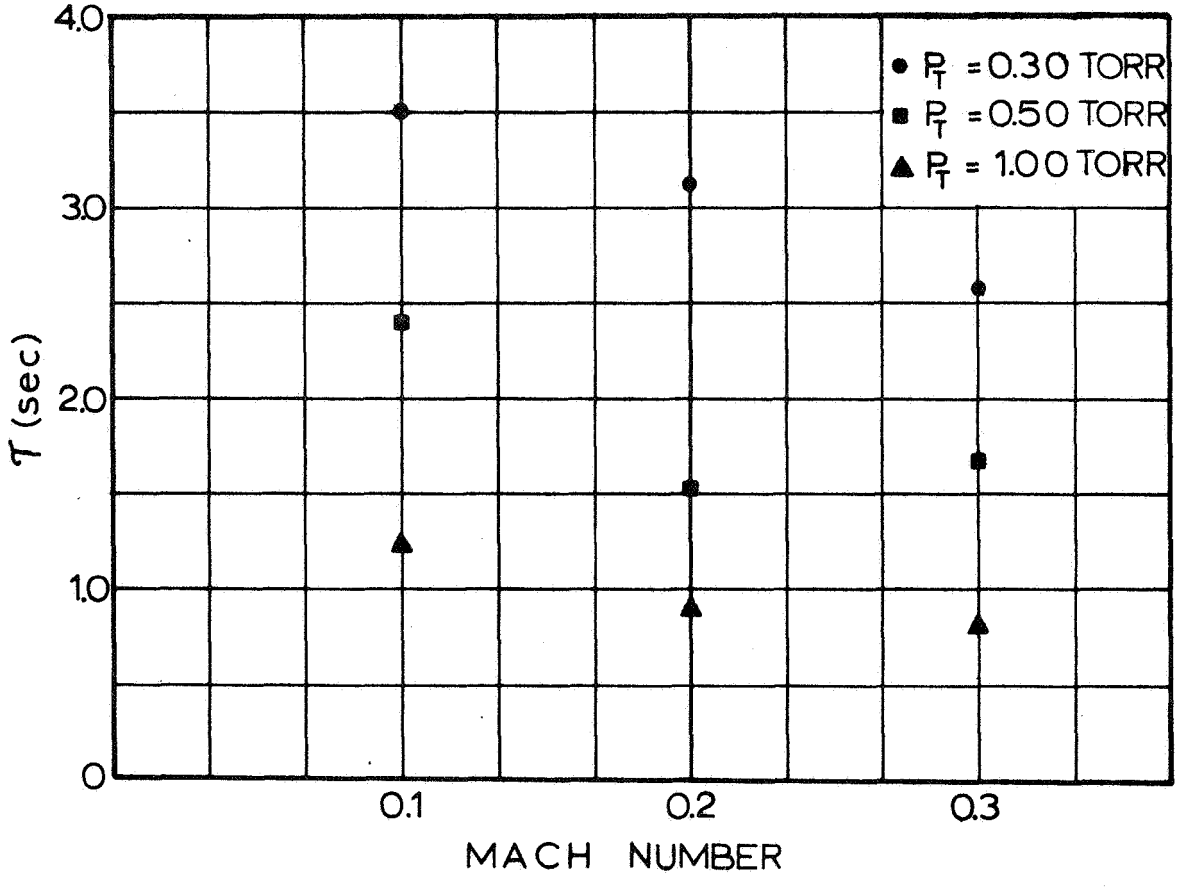

(b)

Fig 14 Sample Response Time Trace and Results of the Response Time Tests

TABLE 1.- RESPONSE TIME TEST CONDITIONS AND RESULTS

M	P_T(torr)	R_I(ohm)	T_I(C)	R_E(ohm)	T_E(C)	T(C)	τ(sec)
0.10	0.30	3780	51.78	10268	23.70	34.03	3.51
	0.50	3720	52.11	9724	25.12	35.05	2.39
	1.00	1890	73.67	8942	27.30	44.36	1.22
0.20	0.30	2195	68.69	8908	27.42	42.60	3.12
	0.50	2470	64.89	9180	26.63	40.70	1.51
	1.00	2530	64.11	9452	25.87	39.93	0.88
0.30	0.30	2700	62.05	8636	28.26	40.69	2.58
	0.50	2700	62.05	8976	27.22	40.03	1.66
	1.00	2770	61.28	9520	25.68	38.77	0.80

TABLE 2.- EXPERIMENTAL DATA

M	P_T(torr)	Re	K	R_E(ohms)	T_E (C)	R_T(ohms)	T_T (C)	r	α(deg)
0.10	0.50	0.369	0.404	9625	25.39	10225	25.40	0.991	0
↓	0.70	0.516	0.289	9605	25.44	10230	25.39	1.093	
0.15	0.50	0.548	0.408	9565	25.55	10210	25.44	1.083	
↓	0.70	0.767	0.291	9610	25.43	10250	25.35	1.058	
0.20	0.51	0.737	0.404	10380	23.42	11100	23.26	1.069	
↓	0.70	1.011	0.295	10260	23.73	10940	23.63	1.043	
0.25	0.51	0.907	0.411	10410	23.34	11140	23.16	1.048	
↓	0.70	1.245	0.299	10270	23.70	10955	23.59	1.030	
0.30	0.30	0.628	0.712	9160	26.69	9870	26.32	1.071	
	0.40	0.837	0.533	9540	25.63	10270	25.28	1.067	
	0.40	0.837	0.533	9200	26.57	9890	26.27	1.059	
	0.50	1.047	0.427	9260	26.40	9930	26.16	1.046	
	0.60	1.255	0.356	9630	25.38	10310	25.18	1.038	
	0.60	1.255	0.356	9315	26.25	9950	26.11	1.027	
	0.70	1.468	0.305	9360	26.11	9965	26.07	1.008	
	0.80	1.674	0.267	9720	25.14	10350	25.08	1.011	
	0.80	1.674	0.267	9395	26.03	9985	26.02	1.001	
	0.90	1.884	0.237	9430	25.92	10000	25.98	0.988	
	1.00	2.093	0.213	9780	24.98	10375	25.02	0.991	
	1.00	2.093	0.213	9455	25.86	10010	25.95	0.982	
	1.10	2.302	0.194	9800	24.93	10380	25.00	0.986	
	1.10	2.302	0.194	9480	25.79	10020	25.93	0.972	
	1.30	2.740	0.164	9840	24.82	10400	24.96	0.974	
	1.30	2.740	0.164	9510	25.70	10035	25.89	0.963	
	1.50	3.139	0.143	9865	24.75	10400	24.96	0.961	
	1.50	3.139	0.143	9530	25.66	10035	25.89	0.955	
	1.70	3.558	0.125	9870	24.74	10400	24.96	0.959	

TABLE 2.- EXPERIMENTAL DATA - Continued

M	P_T(torr)	Re	K	R_E(ohms)	T_E (C)	R_T(ohms)	T_T (C)	r	α(deg)
0.30	1.70	3.558	0.125	9535	25.64	10035	25.89	0.951	0
	2.00	4.186	0.107	9865	24.75	10380	25.00	0.952	
	2.00	4.186	0.107	9530	25.65	10015	25.94	0.944	
	2.50	5.232	0.085	9820	24.88	10325	25.14	0.949	
	2.50	5.232	0.085	9480	25.78	9960	26.09	0.940	
	3.00	6.279	0.071	9760	25.04	10270	25.28	0.950	
	3.00	6.279	0.071	9420	25.96	9905	26.22	0.948	
	3.50	7.325	0.061	9710	25.17	10210	25.44	0.946	
	3.50	7.325	0.061	9360	26.11	9840	26.40	0.944	
	4.00	8.372	0.054	9650	25.33	10140	25.62	0.944	
	4.00	8.372	0.054	9300	26.28	9775	26.58	0.943	
	4.50	9.418	0.048	9590	25.49	10080	25.77	0.956	
	4.50	9.418	0.048	9240	26.46	9710	26.74	0.944	
	5.00	10.465	0.043	9530	25.65	10020	25.93	0.945	
	5.00	10.465	0.043	9170	26.67	9650	26.91	0.952	
0.10	0.24	0.177	0.842	10550	22.99	11175	23.08	0.851	-10
				10525	23.05	11150	23.14	0.851	-10
				10550	22.99	11180	23.08	0.860	0
				10545	23.01	11170	23.10	0.851	0
				10530	23.04	11150	23.14	0.832	0
				10520	23.07	11145	23.15	0.860	0
				10545	23.01	11170	23.10	0.851	+10
				10535	23.01	11155	23.13	0.791	+10
				10550	22.99	11165	23.11	0.804	+20
				10550	22.99	11160	23.12	0.785	+20
				10565	22.97	11160	23.12	0.738	+30
				10555	22.98	11145	23.15	0.710	+30

TABLE 2.- EXPERIMENTAL DATA - Continued

M	P_T(torr)	Re	K	R_E(ohms)	T_E (C)	R_T(ohms)	T_T (C)	r	α(deg)
0.10	0.50	0.369	0.404	9925	24.60	10530	24.63	0.944	-10
	↓	↓	↓	9905	24.66	10510	24.68	0.963	-10
	↓	↓	↓	9920	24.62	10530	24.63	0.972	0
	0.51	0.376	0.396	9905	24.66	10510	24.68	0.963	0
	0.50	0.369	0.404	9920	24.62	10525	24.64	0.953	+10
	0.51	0.376	0.396	9910	24.64	10510	24.68	0.935	+10
	↓	↓	↓	9930	24.58	10520	24.66	0.879	+20
	↓	↓	↓	9920	24.62	10510	24.68	0.897	+20
	↓	↓	↓	9935	24.57	10515	24.67	0.841	+30
	0.50	0.369	0.404	9925	24.60	10500	24.71	0.822	+30
	0.98	0.723	0.206	10845	22.30	11525	22.29	1.009	-10
	0.99	0.730	0.204	10825	22.35	11500	22.35	1.000	-10
	1.00	0.737	0.202	10845	22.30	11520	22.31	0.981	0
	1.00	0.737	0.202	10845	22.30	11525	22.29	1.009	0
	0.99	0.730	0.204	10825	22.35	11500	22.35	1.000	0
	0.98	0.723	0.206	10840	22.31	11520	22.31	1.000	+10
	↓	↓	↓	10830	22.33	11505	22.34	0.991	+10
	↓	↓	↓	10845	22.30	11510	22.33	0.953	+20
	↓	↓	↓	10840	22.31	11510	22.33	0.972	+20
	↓	↓	↓	10855	22.28	11510	22.33	0.915	+30
	0.99	0.730	0.204	10840	22.31	11500	22.35	0.934	+30
0.15	0.25	0.274	0.815	10010	24.38	10690	24.24	1.104	-10
	↓	↓	↓	10005	24.40	10670	24.29	1.083	-10
	↓	↓	↓	10000	24.41	10660	24.31	1.070	-10
	↓	↓	↓	10020	24.35	10710	24.18	1.124	0
	↓	↓	↓	10005	24.40	10670	24.29	1.083	0
	↓	↓	↓	9995	24.42	10660	24.31	1.083	0

TABLE 2.- EXPERIMENTAL DATA - Continued

M	P_T(torr)	Re	K	R_E(ohms)	T_E (C)	R_T(ohms)	T_T (C)	r	α(deg)
0.15	0.25	0.274	0.815	10010	24.38	10670	24.29	1.066	+10
				10015	24.37	10660	24.31	1.046	+20
				10020	24.35	10675	24.27	1.062	+20
	0.24	0.263	0.849	10025	24.33	10690	24.24	1.066	+20
	0.25	0.274	0.815	10050	24.27	10700	24.21	1.046	+30
	0.24	0.263	0.849	10040	24.30	10685	24.24	1.041	+30
	0.50	0.548	0.407	9925	24.60	10580	24.51	1.066	-10
				9910	24.64	10560	24.56	1.062	-10
				9930	24.58	10580	24.51	1.054	0
				9920	24.62	10575	24.52	1.070	0
				9935	24.57	10590	24.48	1.070	+10
				9920	24.62	10570	24.53	1.066	+10
				9945	24.55	10595	24.47	1.062	+20
				9925	24.60	10570	24.53	1.054	+20
				9965	24.50	10600	24.46	1.033	+30
				9940	24.56	10565	24.54	1.012	+30
	1.00	1.096	0.204	10870	22.24	11540	22.27	0.979	-10
				10840	22.31	11510	22.33	0.985	-10
				10870	22.24	11540	22.27	0.979	0
				10870	22.24	11535	22.27	0.975	0
				10870	22.24	11540	22.27	0.979	+10
				10865	22.26	11530	22.28	0.983	+10
				10860	22.27	11530	22.28	0.987	+20
	0.98	1.074	0.208	10875	22.23	11545	22.26	0.979	+20
	0.99	1.085	0.206	10885	22.21	11545	22.26	0.967	+30
				10860	22.27	11525	22.29	0.979	+30
				10855	22.28	11515	22.31	0.975	+30

TABLE 2.- EXPERIMENTAL DATA - Continued

M	P_T(torr)	Re	K	R_E(ohms)	T_E (C)	R_T(ohms)	T_T (C)	r	α(deg)
0.20	0.25	0.361	0.825	10205	23.88	10940	23.63	1.107	-10
				10160	23.99	10880	23.77	1.092	-10
				10200	23.89	10930	23.66	1.099	0
				10190	23.91	10920	23.68	1.090	0
				10160	23.99	10880	23.77	1.092	0
				10185	23.92	10910	23.70	1.092	+10
				10165	23.97	10885	23.77	1.088	+10
				10190	23.91	10905	23.72	1.080	+20
				10180	23.93	10890	23.75	1.078	+20
				10200	23.89	10895	23.73	1.066	+30
				10185	23.92	10870	23.79	1.052	+30
	0.50	0.722	0.412	10110	24.11	10825	23.90	1.090	-10
				10125	24.08	10835	23.88	1.088	-10
				10125	24.08	10840	23.87	1.092	0
				10120	24.09	10830	23.89	1.085	0
				10125	24.08	10840	23.87	1.092	+10
				10115	24.10	10830	23.89	1.090	+10
	0.51	0.737	0.404	10130	24.07	10845	23.86	1.090	+20
				10110	24.11	10825	23.90	1.090	+20
				10135	24.06	10850	23.84	1.090	+30
				10120	24.09	10825	23.90	1.080	+30
	1.00	1.444	0.206	10890	22.19	11550	22.24	0.981	-10
	1.01	1.458	0.204	10860	22.27	11515	22.31	0.981	-10
	1.00	1.444	0.206	10895	22.18	11550	22.24	0.974	0
	1.01	1.458	0.204	10875	22.23	11525	22.29	0.971	0
	1.00	1.444	0.206	10885	22.21	11545	22.26	0.981	+10
	1.00	1.444	0.206	10870	22.24	11525	22.29	0.976	+10

TABLE 2.- EXPERIMENTAL DATA - Continued

M	P_T(torr)	Re	K	R_E(ohms)	T_E (C)	R_T(ohms)	T_T (C)	r	α(deg)
0.20	1.00	1.444	0.206	10870	22.24	11540	22.27	0.988	+20
	↓	↓	↓	10865	22.26	11530	22.28	0.991	+20
	↓	↓	↓	10860	22.27	11530	22.28	0.993	+30
	1.01	1.458	0.204	10845	22.30	11515	22.31	0.995	+30
0.25	0.25	0.445	0.837	10105	24.13	10850	23.84	1.077	-10
	↓	↓	↓	10095	24.15	10835	23.88	1.074	-10
	↓	↓	↓	10110	24.11	10855	23.83	1.076	0
	↓	↓	↓	10105	24.13	10850	23.84	1.077	0
	↓	↓	↓	10115	24.10	10860	23.82	1.076	+10
	↓	↓	↓	10100	24.14	10840	23.87	1.076	+10
	↓	↓	↓	10120	24.09	10860	23.82	1.073	+20
	↓	↓	↓	10100	24.14	10840	23.87	1.076	+20
	↓	↓	↓	10130	24.07	10865	23.81	1.070	+30
	↓	↓	↓	10110	24.11	10840	23.87	1.067	+30
	0.50	0.889	0.419	10195	23.89	10920	23.68	1.058	-10
	0.52	0.925	0.403	10175	23.94	10905	23.71	1.064	-10
	0.50	0.889	0.419	10210	23.86	10920	23.68	1.049	0
	0.51	0.907	0.411	10190	23.91	10905	23.71	1.053	0
	0.50	0.889	0.419	10190	23.91	10920	23.68	1.061	+10
	0.51	0.907	0.411	10180	23.93	10910	23.70	1.064	+10
	0.50	0.889	0.419	10170	23.96	10920	23.68	1.076	+20
	0.51	0.907	0.411	10165	23.97	10915	23.69	1.076	+20
	0.51	0.907	0.411	10155	24.00	10915	23.69	1.084	+30
	0.52	0.925	0.403	10140	24.04	10905	23.71	1.090	+30
	1.01	1.796	0.207	10850	22.29	11495	22.36	0.980	-10
	↓	↓	↓	10815	22.37	11460	22.44	0.980	-10
	↓	↓	↓	10860	22.27	11500	22.35	0.977	0

TABLE 2.- EXPERIMENTAL DATA - Continued

M	P_T(torr)	Re	K	R_E(ohms)	T_E (C)	R_T(ohms)	T_T (C)	r	α(deg)
0.25	1.00	1.778	0.209	10845	22.30	11485	22.39	0.975	0
	↓	↓	↓	10850	22.29	11500	22.35	0.983	+10
	↓	↓	↓	10830	22.33	11480	22.39	0.983	+10
	↓	↓	↓	10835	22.32	11500	22.35	0.991	+20
	↓	↓	↓	10805	22.39	11475	22.41	0.997	+20
	↓	↓	↓	10780	22.45	11470	22.42	1.009	+30
↓	1.01	1.796	0.207	10820	22.36	11505	22.34	0.995	+30
0.30	0.30	0.628	0.711	9935	24.57	10685	24.24	1.062	-10
	↓	↓	↓	9930	24.58	10675	24.27	1.061	-10
	↓	↓	↓	9945	24.55	10690	24.23	1.060	0
	↓	↓	↓	9940	24.56	10680	24.26	1.057	0
	↓	↓	↓	9940	24.56	10695	24.22	1.064	+10
	0.31	0.649	0.689	9955	24.52	10710	24.18	1.063	+10
	↓	↓	↓	9930	24.58	10710	24.18	1.076	+20
	↓	↓	↓	9925	24.60	10700	24.21	1.075	+20
	↓	↓	↓	9915	24.62	10705	24.19	1.081	+30
	0.50	1.046	0.427	9995	24.42	10710	24.18	1.044	-10
	↓	↓	↓	9965	24.50	10690	24.23	1.051	-10
	↓	↓	↓	10010	24.37	10710	24.18	1.036	0
	↓	↓	↓	9985	24.44	10690	24.23	1.040	0
	↓	↓	↓	9970	24.48	10700	24.20	1.053	+10
	↓	↓	↓	9960	24.51	10695	24.22	1.055	+10
	↓	↓	↓	9920	24.62	10695	24.22	1.075	+20
	0.49	1.025	0.436	9925	24.60	10700	24.20	1.075	+20
	0.49	1.025	0.436	9890	24.69	10695	24.22	1.090	+30
	0.50	1.046	0.427	9875	24.73	10685	24.24	1.093	+30
↓									

TABLE 2.- EXPERIMENTAL DATA - Concluded

M	P_T(torr)	Re	K	R_E(ohms)	T_E (C)	R_T(ohms)	T_T (C)	r	α(deg)
0.30	1.01	2.114	0.142	10830	22.33	11470	22.42	0.984	-10
	↓	↓	↓	10800	22.40	11440	22.48	0.985	-10
				10845	22.30	11470	22.42	0.978	0
				10820	22.36	11445	22.48	0.977	0
				10820	22.36	11465	22.43	0.986	+10
				10805	22.39	11450	22.46	0.987	+10
				10775	22.46	11455	22.44	1.003	+20
				10770	22.47	11450	22.46	1.002	+20
				10740	22.55	11450	22.46	1.017	+30
	↓	↓	↓	10730	22.57	11435	22.49	1.014	+30